

Exchange Frequencies in the 2D Wigner Crystal

B. Bernu,¹ Ladir Cândido,² and D. M. Ceperley²

¹*Laboratoire de Physique Théorique des Liquides, UMR 7600 of CNRS, Université Pierre et Marie Curie, boîte 121, 4 Place Jussieu, 75252 Paris, France*

²*Department of Physics and NCSA, University of Illinois at Urbana–Champaign, Urbana, Illinois 61801*
(Received 4 August 2000)

Using path integral Monte Carlo we have calculated exchange frequencies as electrons undergo ring exchanges in a “clean” 2D Wigner crystal as a function of density. The results show agreement with WKB calculations at very low density, but show a more rapid increase with density near melting. Remarkably, the exchange Hamiltonian closely resembles the measured exchanges in 2D ³He. Using the resulting multispin exchange model we find the spin Hamiltonian for $r_s \leq 175 \pm 10$ is a frustrated antiferromagnetic; its likely ground state is a spin liquid. For lower density the ground state will be ferromagnetic.

DOI: 10.1103/PhysRevLett.86.870

PACS numbers: 73.21.-b, 75.10.-b

The uniform system of electrons is one of the basic models of condensed matter physics. In this paper, we report on the first exact calculations of the spin Hamiltonian in the low density 2-dimensional Wigner crystal (2DWC) near melting. This system is realized experimentally with electrons confined at semiconductor metal-oxide-semiconductor field-effect transistors (MOSFET’s) and heterostructures [1], and for electrons on the surface of liquid helium [2].

A homogeneous charged system is characterized by two parameters: the density given in terms of $r_s = a/a_0 = (m^*/m\epsilon)(\pi a_0^2 \rho)^{-1/2}$ and the energy in effective Rydbergs $Ry^* = (m^*/m_e \epsilon^2) Ry$ where m^* is the effective mass and ϵ the dielectric constant. Figure 1 summarizes the 2D phase diagram. At low density (large r_s) the potential energy dominates over the kinetic energy and the system forms a perfect triangular lattice, the Wigner crystal [3]. Tanatar and Ceperley [4] determined that melting at zero temperature occurs at $r_s \approx 37 \pm 5$. Recent calculations [5] have shown that the low temperature phase is free of point defects for densities with $r_s \geq 50$ but defects may be present very near melting. At densities for $r_s \geq 100$ the melting is classical, and occurs for temperatures $T_{\text{melt}} = 2Ry^*/(\Gamma_c r_s)$ where $\Gamma_c \approx 137$ [6].

We determine the spin-spin interaction in the Wigner crystal, using Thouless’ [8] theory of exchange. According to this theory, in the absence of point defects, at low temperatures the spins will be governed by a Hamiltonian of the form:

$$\mathcal{H}_{\text{spin}} = - \sum_P (-1)^P J_P \hat{P}_{\text{spin}}, \quad (1)$$

where the sum is over all cyclic (ring) exchanges described by a cyclic permutation P , J_P is its exchange frequency, and \hat{P}_{spin} is the corresponding spin exchange operator. Path integral Monte Carlo (PIMC) as suggested by Thouless [8] and Roger [9] has proved to be the only reliable way to calculate these parameters. The theory and computational method have been tested thoroughly on the

magnetic properties of bulk helium obtaining excellent agreement with measured properties [10]. Rather surprisingly, it has been found [11] that in both 2D and 3D solid ³He, exchanges of two, three, and four particles have roughly the same order of magnitude and must all be taken into account. This is known as the multiple spin exchange (MSE) model.

A WKB calculation of the exchange frequencies in the 2DWC by Roger [9] predicted that the three electron J_3 nearest neighbor exchange would dominate, leading to a ferromagnetic (F) ground state. Recent calculations [12,13] have confirmed and extended those of Roger. Although the $1/r$ interaction is characterized as “soft,” in

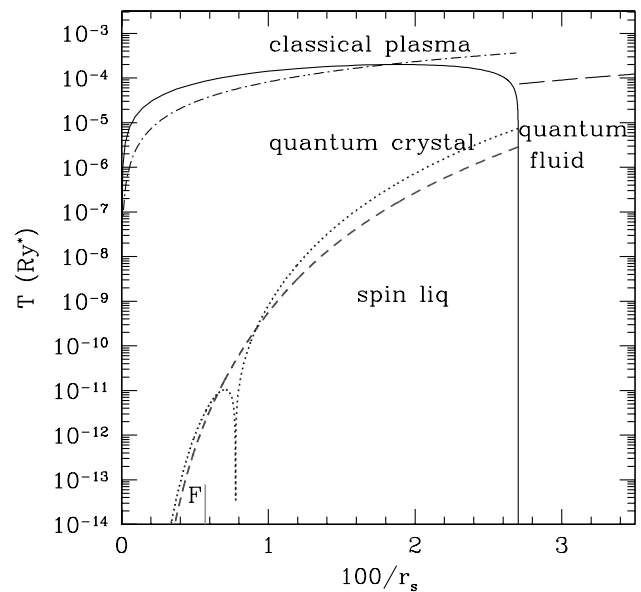


FIG. 1. Phase diagram. The estimated melting line is based on Lindemann’s criteria [7]. The dash-dotted line represents the Debye temperature. The dotted line is the Curie-Weiss constant θ , and the dashed line is the coefficient J_c of the specific heat at high temperature as defined in the text. The vertical line is the estimated zero temperature ferromagnetic (F) transition.

the 2DWC the two particle pair correlation function for the electron system is quite similar to that of solid ^3He supporting the idea that multiple exchanges could be important in the 2DWC near melting.

An exact method for calculating the exchange frequency in quantum crystals has been previously developed and applied to solid ^3He [10,14,15]. One computes the free energy necessary to make an exchange beginning with one arrangement of particles to lattice sites Z and ending on a permuted arrangement PZ :

$$F_P(\beta) = Q(P, \beta)/Q(I, \beta) = \tanh[J_P(\beta - \beta_0)]. \quad (2)$$

Here $Q(P, \beta)$ is the partition function corresponding to an exchange P at a temperature $1/\beta$. I is the identity permutation. Note that these paths are of “distinguishable” particles since Fermi statistics are implemented through the spin Hamiltonian in Eq. (1). We determine the function $F_P(\beta)$ using a method which directly calculates free energy differences and thereby determines J_P and β_0 . The only new feature with respect to the ^3He calculations is the method of treating the long-range potential. We use the standard Ewald breakup [9] and treat the short-range part using the exact pair action [10] and the long-range k -space term using the primitive approximation. We used a hexagonal unit cell with periodic boundary conditions, with most calculations containing 36 electrons. Checks with up to 144 electrons did not change the results within the statistical errors. The number of particles is not as important in the 2DWC as in solid ^3He because the $1/r$ interaction suppresses the long wavelength charge fluctuations.

We performed calculations for the densities $r_s = \{45, 50, 60, 75, 100, 140, \text{ and } 200\}$. We found accurate results using a “time step” for the discretized imaginary time path integrals of $\tau \leq 0.3r_s^{3/2}$ and extrapolated to the $\tau = 0$ limit using $J_p(\tau) = J_p(0) + J'_p \tau^3$. The inverse temperature β in Eq. (2) must be larger than the values determined by melting and twice the exchange “time” $\beta_0 \sim 5r_s^{3/2}$. We have determined the exchange frequencies with an accuracy between 1.5% and 6% independent of their magnitude or the number of exchanging electrons, though the computer time increases with the number of exchanging electrons. Breakdown of Thouless’ theory caused by many states contributing to the ratio of partition functions would be signaled by $F_P(\beta)$ not described by Eq. (2). Except for $r_s < 50$, where our calculations are too unstable to make definite predictions, we observed no problems of convergence.

Figure 2 shows the ring exchanges considered here. Except near melting, these exchanges give rise to most of the thermodynamic properties. Note that we consider the six particle parallelogram ($6p$) exchange, which is not taken into account in solid ^3He . We have also calculated several 2–5 particle exchanges having next nearest neighbor exchanges and all possible six particle nearest neighbor exchanges for $50 \leq r_s \leq 75$, but because their magnitudes are much smaller, we do not report those results.

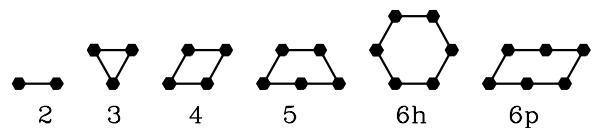


FIG. 2. Considered exchanges.

Our calculated exchange frequencies vary rapidly with density as shown in Fig. 3. One can see that they are much less than the zero point energy of the electrons, thus justifying the use of Thouless’ theory. The WKB method [11], where one approximates the path integral in Eq. (2) by the single most probable path, explains most of this density dependence. In the 2DWC, the WKB expression for the exchange frequency [9,12,13] is

$$J_P = A_P(r_s) b_P^{1/2} r_s^{-5/4} e^{-b_P r_s^{1/2}}. \quad (3)$$

Here $b_P r_s^{1/2}$ is the minimum value of the action integral along the path connecting PZ with Z . The three particle exchange exponent is the smallest indicating that as $r_s \rightarrow \infty$, J_3 will dominate and the system will have a ferromagnetic ground state. However, note that in Fig. 3 $J_2 > J_3$ for $r_s \leq 90$.

Figure 4 shows the ratio of the exact frequencies to those from the WKB approximation [13]. We note that the ratios tend to a constant of order unity for large r_s , but a value of ≈ 1.4 for J_2 and J_4 . All the frequencies increase much more rapidly than those of WKB, especially J_5 and J_6 , as the system approaches the melting density because of fluctuations away from the most probable path. Near melting, the spread in exchange frequencies is much less than predicted by WKB resulting in a more highly frustrated spin Hamiltonian.

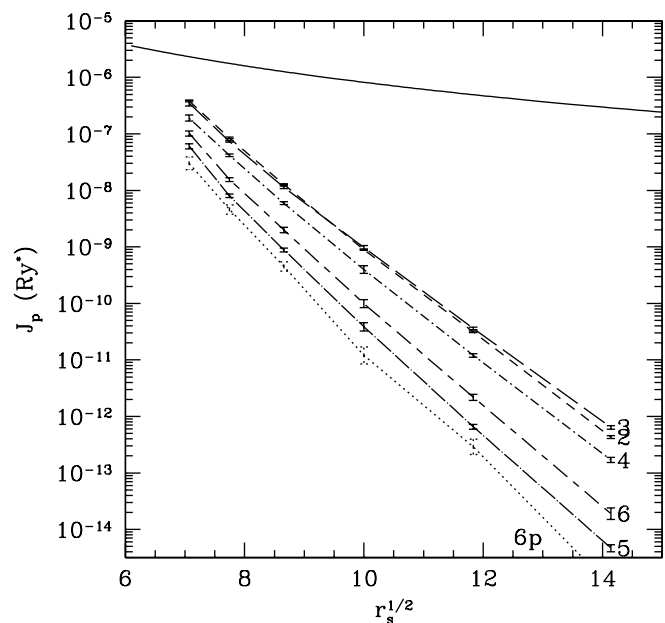


FIG. 3. Exchange frequencies versus $r_s^{1/2}$. The solid line is 10^{-3} of the kinetic energy.

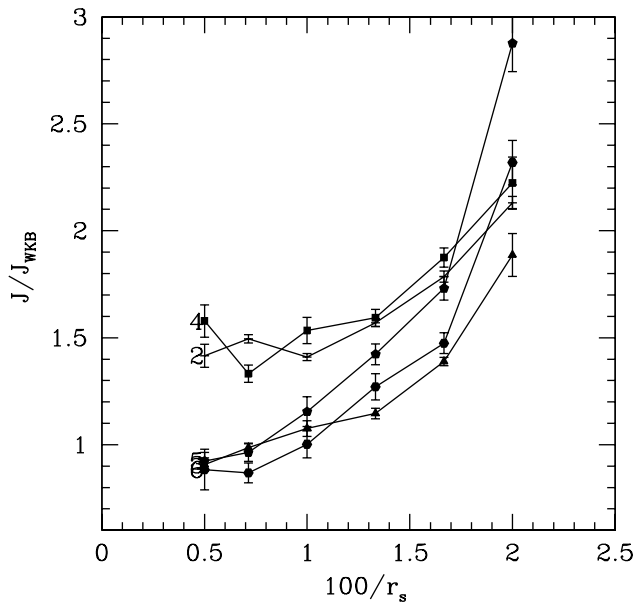


FIG. 4. The ratio of the PIMC exchange frequencies to those from a WKB calculation [13] as a function of density.

We are unaware of any work that definitively establishes the form of the correction to the WKB formula. A good fit was obtained with the function $A_P(r_s) = A_P(0)[1 + (r_P/r_s)^3]$ to determine b_P , $A_P(0)$, and r_P . The exponents are close to the WKB values [13], differing at most by 0.02.

A recent calculation [16] directly evaluates J_2 in the high density regime, $5 \leq r_s \leq 45$, by numerically solving for the difference between the even and odd parity two electron energies. In those calculations, the spectator electrons were fixed at their lattice sites and the two exchanging electrons had vanishing wave functions outside a rectangle centered around the exchange. At $r_s = 45$, a direct comparison shows their result is 2.3 times larger than that obtained with PIMC. This result is expected because of the additional localization caused by the spectator electrons fluctuating into the exchanging region.

Having determined the exchange frequency, one is left with the spin Hamiltonian of Eq. (1). This is a nontrivial many-body problem which we will not discuss in detail here. For spin 1/2 systems, J_2 and J_3 contribute only with a nearest neighbor Heisenberg term: $J_2^{\text{eff}} = J_2 - 2J_3$. This term is negative (ferromagnetic) but approaches zero near melting. For convenience we use J_4 as a reference to fix the overall scale of the magnetic energy. Neglecting J_{6p} , the Hamiltonian has three remaining parameters J_2^{eff}/J_4 , J_5/J_4 , and J_{6h}/J_4 . The dependence of these ratios on density is shown in Fig. 5.

High temperature series expansions [17] determine the specific heat C_V and magnetic susceptibility χ_0/χ for temperatures $k_B T \gg J_P$. The susceptibility is given by $\chi_0/\chi = T - \theta + B/T \dots$ and the specific heat $C_V/Nk_B = (3J_c/2T)^2 + \dots$, where the Curie-Weiss constant is given by $\theta = -3(J_2^{\text{eff}} + 3J_4 - 5J_5 + 5/8J_{6h} +$

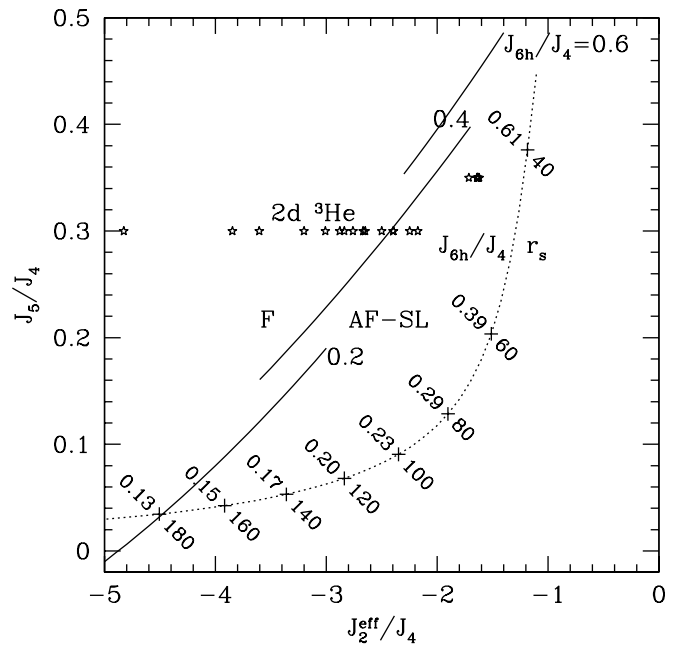


FIG. 5. Spin phase diagram as a function of exchange ratios. The dotted line is the flow of spin Hamiltonian space versus r_s (lower numbers); also shown are the estimated values of J_{6h}/J_4 (upper numbers). The solid lines are the limit of the ferromagnetic phase according to ED [18] at $J_{6h}/J_4 = \{0.2, 0.4, \text{ and } 0.6\}$. The 2DWC crosses into the F region for $r_s \approx 175$. The (*) are empirical estimates of the spin Hamiltonian of 2D ^3He at several densities [20].

$15/4J_{6p})$ with a quadratic expression of the J 's for J_c . These two constants, which set the scale of the temperature where exchange is important, are shown as dotted and dashed lines in Fig. 1. Note that θ changes from positive to negative at $r_s \approx 130$. Both θ and J_c decrease very rapidly at low density showing that experiments must be done at $r_s \leq 60$ if spin effects are to be at a reasonable temperature, e.g. $T_c > 0.1$ mK (assuming the values for Si-MOSFET: $\epsilon = 7.7, m^* = 0.2$).

The zero temperature state can be studied by exact diagonalization (ED) of an N site system. (The present limitation is $N \leq 36$.) Here we summarize the findings from Ref. [18] to characterize the stability of the ferromagnetic (F) phase and the nature of the antiferromagnetic (AF) phase. The F-AF transition is shown in Fig. 5. The ferromagnetic phase is obtained only at very low density: we estimate the F-AF transition for the 2DWC will occur at $r_s = 175 \pm 10$. (Note that this estimate does not include the effect of J_{6p} ; this will increase the stability of the antiferromagnetic region to roughly $r_s = 200$.)

At higher density, the frustration between large cyclic exchanges (4–6 body loops) results in a disordered spin state [18]. For example, the point ($J_2^{\text{eff}}/J_4 = -2, J_5 = 0, J_{6h} = 0$), close to the parameters at $r_s = 100$, is a spin liquid with a gap to all excitations. The spin liquid properties can be understood from a resonance valence bond model with ordering into spin-1 diamond plaquettes. The

TABLE I. Fits for the exchange frequencies. The path area, a_p , was calculated at $r_s = 60$ and it is in units of triangle areas.

P	b_p	$A_p(0)$	r_p	a_p
2	1.612	2.11	44	
3	1.525	0.91	47	2.07(1)
4	1.656	1.42	45	3.07(2)
5	1.912	1.39	60	4.11(2)
$6h$	1.790	1.12	59	7.04(3)
$6p$	2.136	6.24	38	5.09(2)

breakup of the plaquettes is responsible for a low temperature peak on the specific heat. A second high temperature peak develops at a temperature $T \sim J_c$, shown as a dotted line in Fig. 1. However, because this interpretation is based primarily on the analysis of small spin systems, or uses approximate analytical methods and takes into account mainly only two, three, and four spin exchanges [18], one cannot rule out more exotic types of spin order.

We find that at higher densities ($r_s < 100$), the trajectory of the MSE models parallels the F-AF phase line, with the possibility of a reentrant ferromagnetic phase for $r_s < 40$. Note that quantum Monte Carlo calculations [19] of the normal Fermi liquid at $r_s = 30$ show that the ferromagnetic phase has a slightly lower energy than the unpolarized phase. Hence both the high density 2DWC and the low density electron fluid are characterized by a spin Hamiltonian which is nearly ferromagnetic.

We note a remarkable similarity between the exchange parameters of the 2DWC to those extrapolated from measurements of the second layer of ^3He absorbed on grafoil [20] as shown in Fig. 5. The existence of two separate realizations of this frustrated spin Hamiltonian should allow a fuller investigation of the proposed spin liquid state. Such an equivalence could arise from an underlying virtual vacancy-interstitial (VI) mechanism [11] giving rise to ring exchanges. In this model the prefactor of the exchange is controlled by the rate of VI formation (nonuniversal) but the ratios of the various ring exchanges arise from geometry of the triangular lattice and from the attraction of point defects (universal). We have recently determined [5] that the VI formation energy vanishes at melting in the 2DWC. This is consistent with the fact that the various J_p increase rapidly near melting.

In summary, we find that the magnetic interactions are characterized by a frustrated spin order. Application of a magnetic field [21] transforms the exchange frequencies to $J_p e^{2\pi i e B_\perp a_p / h}$ where a_p is the area of the exchange (see Table I) and B_\perp the magnetic field. Experiments with magnetic fields will allow exploration of this Aharonov-Bohm effect and thereby provide direct information on ring exchanges.

The semiconductor realizations of the 2DWC have significant disorder which might stabilize localized electronic

states (a Wigner glass) at higher densities than in the clean system [22]. It has been argued [12] that disorder will favor the spin liquid phase. One can also stabilize the Wigner crystal at higher densities using bilayers [23]. Exchange frequencies in those systems including effects of layer thickness and the exchange properties of point defects could be calculated with the present method.

This research was funded by NSF DMR 98-02373, the CNRS-University of Illinois exchange agreement, support by Fundação de Amparo à Pesquisa do Estado de São Paulo (FAPESP), and the Department of Physics at the University of Illinois. We used the computational facilities at the NCSA.

-
- [1] J. Yoon *et al.*, Phys. Rev. Lett. **82**, 1744 (1999).
 - [2] C. C. Grimes and G. Adams, Phys. Rev. Lett. **42**, 795 (1979).
 - [3] X. Zhu and S. G. Louie, Phys. Rev. B **52**, 5863 (1995).
 - [4] B. Tanatar and D. M. Ceperley, Phys. Rev. B **39**, 5005 (1989).
 - [5] L. Cândido, P. Phillips, and D. M. Ceperley, Phys. Rev. Lett. (to be published).
 - [6] K. Strandburg, Rev. Mod. Phys. **60**, 161 (1988).
 - [7] F. Douchin and D. M. Ceperley (unpublished).
 - [8] D. J. Thouless, Proc. Phys. Soc. London **86**, 893 (1965).
 - [9] M. Roger, Phys. Rev. B **30**, 6432 (1984).
 - [10] D. M. Ceperley, Rev. Mod. Phys. **67**, 279 (1995).
 - [11] M. Roger, J. H. Hetherington, and J. M. Delrieu, Rev. Mod. Phys. **55**, 1 (1983).
 - [12] S. Chakravarty, S. Kivelson, C. Nayak, and K. Voelker, Philos. Mag. B **79**, 859 (1999).
 - [13] M. Katano and D. S. Hirashima, Phys. Rev. B **62**, 2573 (2000).
 - [14] D. M. Ceperley and G. Jacucci, Phys. Rev. Lett. **58**, 1648 (1987).
 - [15] B. Bernu and D. Ceperley, in *Quantum Monte Carlo Methods in Physics and Chemistry*, edited by M. P. Nightingale and C. J. Umrigar (Kluwer, Dordrecht, The Netherlands, 1999).
 - [16] V. V. Flambaum, I. V. Ponomarev, and O. P. Sushkov, Phys. Rev. B **59**, 4163 (1999).
 - [17] M. Roger, Phys. Rev. B **56**, R2928 (1997).
 - [18] G. Misguich, B. Bernu, C. Lhuillier, and C. Waldtmann, Phys. Rev. Lett. **81**, 1098 (1998); G. Misguich, C. Lhuillier, B. Bernu, and C. Waldtmann, Phys. Rev. B **60**, 1064 (1999).
 - [19] D. Varsano, S. Moroni, and G. Senatore, cond-mat/0006397.
 - [20] M. Roger, C. Bauerle, Yu. M. Bunke, A.-S. Chen, and H. Godfrin, Phys. Rev. Lett. **80**, 1308 (1998).
 - [21] S. A. Kivelson *et al.*, Phys. Rev. B **36**, 1620 (1987); T. Okamoto and S. Kawaji, Phys. Rev. B **57**, 9097 (1998).
 - [22] S. T. Chui and B. Tanatar, Phys. Rev. Lett. **74**, 458 (1995).
 - [23] F. Rapisarda and G. Senatore, Aust. J. Phys. **49**, 161 (1996); Int. J. Mod. Phys. B **13**, 479 (1999).